

resolve the validity of their proposed relation.

REFERENCES AND NOTES

1. R. C. Weisenberg and C. Cianci, *J. Cell Biol.* **99**, 1527 (1984).
2. R. C. Weisenberg, R. D. Allen, S. Inoué, *Proc. Natl. Acad. Sci. U.S.A.* **83**, 1728 (1986).
3. R. J. Lasek, J. A. Garner, S. T. Brady, *J. Cell Biol.* **99**, 212s (1984).
4. Abbreviations used: MES, 4-morpholineethanesulfonic acid; DTT, dithiothreitol; MAPs, microtubule-associated proteins; GTP, guanosine 5'-triphosphate.
5. B. M. Riederer, I. S. Zagon, S. R. Goodman, *J. Cell Biol.* **102**, 2008 (1986).
6. M. Tytell, S. T. Brady, R. J. Lasek, *Proc. Natl. Acad. Sci. U.S.A.* **81**, 1570 (1984).
7. G. Huber and A. R. Matus, *J. Neurosci.* **4**, 151 (1984); A. R. Matus, R. Bernhardt, T. Hugh-Jones, *Proc. Natl. Acad. Sci. U.S.A.* **78**, 3010 (1981).
8. ATPase activities were determined by measuring phosphate release according to the method of J. K. Heinonen and R. J. Lahti [*Anal. Biochem.* **113**, 313 (1981)].
9. M. S. Runge, W. W. Schaeffer, R. C. Williams, Jr., *Biochemistry* **20**, 170 (1981).
10. R. V. Zackroff and R. D. Goldman, *Science* **208**, 1152 (1980).
11. D. B. Murphy, K. T. Wallis, R. R. Hiesch, *J. Cell Biol.* **96**, 1306 (1983).
12. G. M. Langford, R. D. Allen, D. G. Weiss, *Cell Motil. Cytoskeleton* **7**, 20 (1987).
13. T. Lorenz and M. Willard, *Proc. Natl. Acad. Sci. U.S.A.* **75**, 505 (1978).
14. M. Black and R. J. Lasek, *J. Cell Biol.* **86**, 616 (1980).
15. Y. Komiya and M. Kurokawa, *Brain Res.* **190**, 505 (1980).
16. Y. Komiya, *Neurobiology* **14**, 87 (1983).
17. I. G. McQuarrie, S. T. Brady, R. J. Lasek, *J. Neurosci.* **6**, 1593 (1986).
18. S. T. Brady, M. Tytell, R. J. Lasek, *J. Cell Biol.* **99**, 1716 (1984).
19. B. Grafstein, B. S. McEwen, M. L. Shelanski, *Nature (London)* **227**, 289 (1970).
20. T. Tashiro, M. Kurokawa, M. Komia, *J. Neurochem.* **43**, 1120 (1984).
21. G. Filliatreau and L. De Giambardino, *ibid.* **44**, s122 (1985).
22. T. Tashiro and Y. Komiya, *Biomed. Res.* **4**, 443 (1983).
23. R. A. Nixon and K. Logvinenko, *J. Cell Biol.* **102**, 647 (1986).
24. P. N. Hoffman, J. W. Griffin, D. L. Price, *ibid.* **99**, 705 (1984).
25. J. R. Bamburg, D. Bray, K. Chapman, *Nature (London)* **321**, 788 (1986).
26. To isolate pure tubulin and SCAPs, we centrifuged crude microtubule proteins in a Beckman 65 rotor at 45,000 rev/min (175,000g) for 15 minutes at 4°C. The supernatant, containing free tubulin, and the pellet, containing SCAPs, were recovered. The supernatant was applied to a slurry of phosphocellulose, equilibrated with MES-DTT buffer, in a double centrifuge tube. The unbound protein, containing nearly pure tubulin, was recovered by centrifugation in a table-top centrifuge. To isolate SCAPs, we rinsed the pellet from the 175,000g centrifugation gently with MES-DTT buffer containing 1M NaCl and 10% glycerol (in some experiments 1% Triton X-100 was included) and then resuspended it in the same buffer. The dispersed pellet was layered on top of a cushion (2 to 3 ml) of MES buffer made up to 25% glycerol and centrifuged in a Beckman 65 rotor at 45,000 rev/min for 15 minutes at 4°C. The pellet, containing the purified SCAPs, was rinsed gently in MES-DTT buffer plus 15% glycerol and was resuspended and homogenized in the same buffer. The homogenized pellet was further dispersed by sonication for 1 to 2 seconds in a Braunsonic model 1510 sonicator operated at 100 W. Although for all the experiments reported here we used SCAPs isolated from crude microtubule proteins, SCAPs were also isolated directly from brain
27. Supported by grants from the National Institutes of Health and the American Diabetes Association to R.C.W. We thank C.-S. Nic for assistance. The MAP2 antibody was a gift from A. R. Matus.

4 February 1987; accepted 11 June 1987

Nerve Terminal Remodeling Visualized in Living Mice by Repeated Examination of the Same Neuron

DALE PURVES, JAMES T. VOYVODIC, LORENZO MAGRASSI, HIROMU YAWO

The distribution of presynaptic endings on the surfaces of autonomic ganglion cells was mapped in living mice after intravenous administration of a styryl pyridinium dye. The staining and imaging techniques did not appear to damage the ganglion cells, or the synapses on them; these procedures could therefore be repeated after an arbitrary period. Observations of the same neurons at intervals of up to 3 weeks indicate that the pattern of preganglionic terminals on many of these nerve cells gradually changes.

WHETHER THE ARRANGEMENT OF nerve terminals on target neurons in the mammalian nervous system is normally stable or continually changing is not known. This issue is important because it bears on the way the adult nervous system generates long-term change. The development of nontoxic fluorescent dyes, low light level video cameras, and digital image processing has made it possible to observe pre- and postsynaptic processes over time in living animals (1). Using these methods in the peripheral nervous system of the mouse, we have studied the long-term stability of sympathetic ganglion cell dendrites (postsynaptic elements) (2, 3) and the stability of motor nerve terminals at neuromuscular junctions (4, 5). We now report on the stability of nerve terminals of central neurons on the cell bodies of parasympathetic ganglion cells.

A saline solution (0.2 to 0.3 ml; 1 mM) of 4-(4-dimethylaminostyryl)-N-methylpyridinium iodide (4-Di-1-ASP) (Molecular Probes Inc.) was slowly injected into a tail vein of adult male mice (CF1 strain; 25 to 35 g; 2 to 4 months of age). After 30 to 60 minutes, the animals were anesthetized by intraperitoneal injection of diazepam (0.5 mg/kg), followed by ketamine hydrochloride (1.5 mg/kg), producing surgical anesthesia in 2 to 3 minutes. A satisfactory anesthetic level was maintained for approxi-

mately 45 minutes. An anesthetized mouse was placed on a microscope stage that was modified so that the area of interest could be visualized with either a low-power dissecting lens or higher power compound objectives (2, 3, 5, 6). All work (except the actual imaging of synapses) was carried out in yellow light (510-nm high-pass filter) to minimize irradiation of the cells with wavelengths that excite the dye (peak absorption in water, 494 nm).

A ventral midline incision in the neck exposed the sublingual and submandibular salivary glands and ducts on the right side. Throughout the procedure the wound was perfused with sterile saline (1 to 2 ml per minute; lactated Ringer's solution); positive pressure ventilation was used to control the animal's breathing. The salivary ducts and their associated ganglia were lifted away from the underlying tissues with a highly polished, chrome-plated support. In mice, several parasympathetic ganglia, each comprising up to several hundred nerve cells, are distributed along the ducts (6). An advantage of these particular ganglia is their accessibility. Furthermore, because the neurons lack dendritic processes (7, 8), synaptic contacts occur directly on the cell bodies, where nerve-terminal patterns can be more readily discerned than on complex dendritic arbors.

We selected a region on the surface of one of the ganglia in which the cells were well defined; light reflecting from the chrome-plated support revealed the superficial cells by virtue of asymmetric illumination con-

Department of Anatomy and Neurobiology, Washington University School of Medicine, 660 South Euclid Avenue, St. Louis, MO 63110.

trast (3, 6). Excitation and barrier filters appropriate for 4-Di-1-ASP were then introduced (Leitz H2 system), and the yellow filter was removed from in front of the light source (50 W Hg). The intensity of the illuminating light was controlled by a continuously variable neutral density filter inserted into the light pathway just behind the field diaphragm. Further images were obtained by means of a low light level video camera (GE SIT model 4TE) connected to an image processing system (Recognition Concepts Trapix 5500 running on a DEC MicroVAX II computer) (1, 9).

To visualize fluorescent nerve endings on

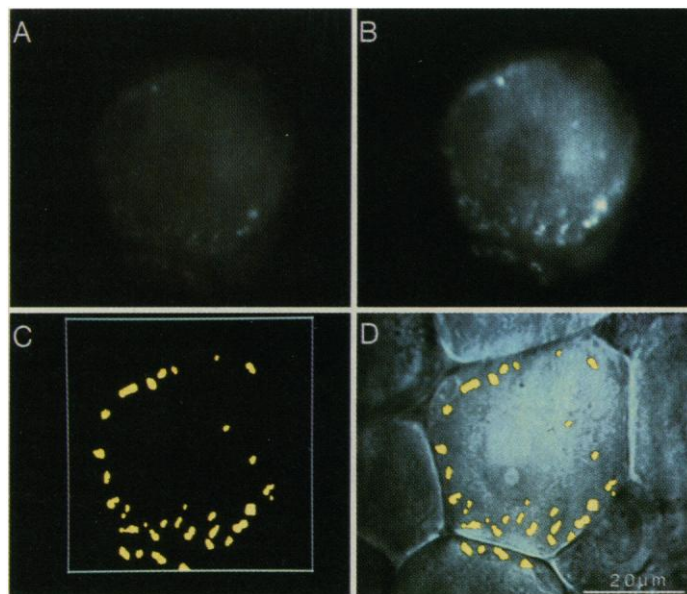
identified ganglion cells, we gradually increased the intensity of the exciting light by adjusting the neutral density filter until a satisfactory image could just be seen on a video screen monitoring the continuously digitized image. One or two cells were selected for detailed study. A focus-through series of images was obtained in a few seconds and stored on a disk for later processing. The total exposure of the stained terminals to the exciting light was minimal (approximately 10 to 15 seconds). After recording the fluorescence pattern on the cell surface in this way, the yellow filter was reinserted into the light pathway, and a

surface image of the neuron of interest and its immediate neighbors was obtained. Additional images were collected at lower magnifications to facilitate reidentification of the same cell at a later time. The wound was then closed. After gentle warming and inhalation of 100% oxygen for an additional half hour, most animals recovered without incident. The stored video images were subsequently processed to produce a composite map of the pattern of fluorescent staining on the neuron of interest (Fig. 1).

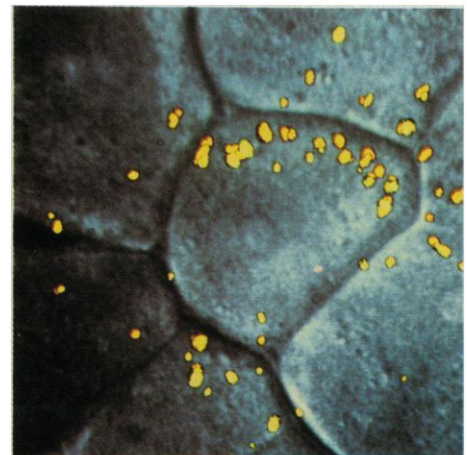
Table 1. Measurement of the electrical properties of ganglion cells and their synaptic responses approximately 1 hour after 4-Di-1-ASP staining by intravenous administration. Neurons were impaled with KCl-filled electrodes having resistances of 60 to 120 megohms. Values are given as means (\pm SEM). The half-maximal decay time of the postsynaptic response is denoted by $t_{1/2}$.

No. of animals	No. of cells examined	Resting potential (mV)	Action potential amplitude (mV)	Amplitude of the postsynaptic response (mV)	$t_{1/2}$ (msec)
4	18	49.8 \pm 1.1	<i>Normal animals</i>		17.3 \pm 2.4
			70.7 \pm 2.0	36.7 \pm 1.7	
7	21	49.8 \pm 1.4	<i>Dye-injected animals</i>		18.7 \pm 1.6
			71.0 \pm 1.4	40.8 \pm 1.7	

Fig. 1. Image processing procedures used to enhance and combine the primary SIT camera images to make fluorescent maps of the surfaces of ganglion cells after vital staining with 4-Di-1-ASP. To maximize the contrast, the field diaphragm was stopped down to a diameter just larger than the outline of the cell of interest. With a $\times 50$ water-immersion objective (numerical aperture, 1.00), the depth of focus is limited to a few micrometers; consequently, images at several different focal planes (usually four) are required to capture all of the putative synapses



on the upper surface of a typical neuron. The focus-through series was always begun at the uppermost surface of the cells and traversed a vertical distance of 10 to 15 μm . (A) Single plane from a focus-through series. Even though 32 frames have been averaged, little detail can be seen without further image processing. (B) The same primary image after contrast enhancement. (C) The same field after further image processing to detect the areas of maximum fluorescent intensity. This procedure uses a contrast-detection convolution to pick out spots more than 20% brighter than background, followed by filtration to remove single pixel noise. The result is a new image that corresponds to the fluorescent spots in the original scene; the box in this and subsequent figures indicates the portion of the original image processed in this way. (D) In this panel, the fluorescent spots in (C), plus three other focal planes, have been superimposed on a surface image of the cell. The fluorescence map is aligned on the surface view by comparison with the original images [see (B) for example]; the fluorescent spots are arbitrarily colored yellow and given a one-pixel-wide black border to make them stand out. The result is a composite map of the regions of maximum fluorescence on a bright-field image of the neuron of interest and its immediate neighbors. Because the field diaphragm is stopped down to a circle just larger than the neuron of interest (see above), synapses on most of the neighboring cells in this and subsequent figures are not apparent.



20 μm

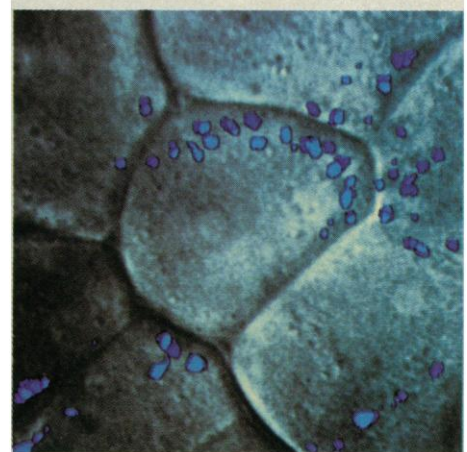


Fig. 2. Fluorescence map of putative preganglionic terminals stained with 4-Di-1-ASP compared with methylene blue-stained synaptic boutons on the same ganglion cell. (Top) Fluorescence map after vital staining with 4-Di-1-ASP (as in Fig. 1). (Bottom) Subsequent image of the same neuron 2 to 3 minutes after in situ staining with methylene blue (6). The methylene blue map was also obtained by the procedure described in Fig. 1, except that negative images of the methylene blue-stained cell were used. Comparison of the distribution of maximum fluorescence intensities and conventionally stained boutons on the same neuron shows good correspondence. Minor differences in the two maps arise because fluorescence staining does not reveal the finest elements in the terminal arbor, whereas methylene blue tends to over stain synaptic endings. Methylene blue also begins to stain nonsynaptic elements after a few minutes of exposure to the dye (6).

To examine the configuration of presynaptic endings on the same cell at a later time, this procedure was repeated after various intervals. The cell of interest was located by reference to the initial images. The second set of fluorescence images was then compared to the original. Differences between the maps were quantitated by graphic analysis (see below).

Normally, up to several dozen terminal boutons with conventional synaptic morphology can be demonstrated on these and other mammalian parasympathetic ganglion cells with histological stains such as methylene blue, zinc iodide-osmium, horseradish peroxidase, or by means of electron microscopy (6, 8, 10, 11). On these mouse neurons, many of the synapses were clustered around the circumference of the cell when it was viewed from the ganglionic surface, often near satellite cell nuclei; some synaptic

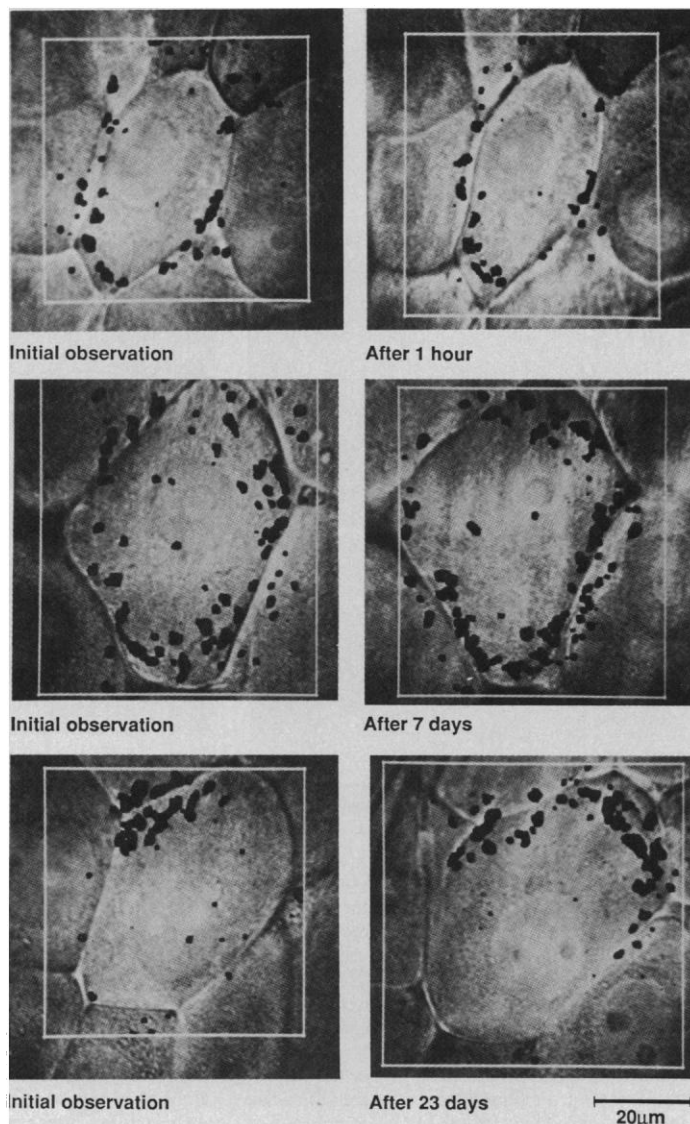
endings were found on the domes of the cells as well. Thus one indication that systemic injection of 4-Di-1-Asp selectively stains synaptic boutons—or structures closely associated with them—was the general appearance and distribution of fluorescent spots after vital staining (Fig. 1). Two additional findings confirmed that the stained structures were presynaptic terminals. First, the fluorescent spots were no longer apparent 3 to 5 days after crushing the preganglionic nerves (ten animals). After denervation, some faintly fluorescent structures could still be seen with illumination of higher intensity than we normally used, but these elements were within the cytoplasm of neurons and overlying connective tissue cells. Second, counterstaining with methylene blue—the traditional histochemical stain for synaptic boutons in autonomic ganglia—showed good correspondence between fluorescent

profiles and methylene blue-stained boutons in each of 42 cells (23 animals) (Fig. 2). This result also indicates that the 4-Di-1-ASP consistently stains most or all of the synaptic endings on these neurons. However, we do not know the mechanism of 4-Di-1-ASP staining, nor do we know the subcellular compartment in which the dye resides.

To determine the degree to which synapses on ganglion cells might be damaged by staining or illumination, several electrophysiological tests were carried out. Twenty-one neurons in ganglia from seven animals were impaled with a microelectrode after vital staining. No obvious differences were observed among stained and unstained preparations in any of several electrical properties that were measured (Table 1). The same result was observed among 12 additional neurons in which synaptic potentials were examined before and after illumination of the stained synapses for 1 minute. By these criteria, the function of the preganglionic terminals was not affected by staining, even after strong illumination for a period several times longer than that normally required to image the pattern of synaptic terminals on the cell surface.

We next assessed the reliability of our mapping procedure by comparing two composite images of the same region obtained acutely, at intervals that we judged to be too brief for any substantial biological change to occur. When we compared two sets of focus-through images obtained just a few seconds apart, the composite maps of the presumptive synaptic endings were always very similar. Slight differences between such images arise because the two series of focal planes are never taken at exactly the same levels. Some degree of error is therefore inherent in our method of imaging. Next, we imaged synaptic endings on the surface of an identified ganglion cell, closed the wound, removed the animal from the microscope stage, and returned it to its cage. After about an hour we reanesthetized the animal, found the same cell, and repeated the imaging procedure (Fig. 3, top). (In this circumstance further administration of dye was not necessary because substantial amounts of 4-Di-1-ASP remain in the animal's blood and tissues for several hours.) Thus we examined the degree to which the original synaptic map would differ from a later one simply as a result of the deformation of the neurons (and the synapses on them) that arises from mechanical forces on the tissue (the deformation of a ganglion and its constituent cells will not be exactly the same when the neuron of interest is exposed and imaged a second time). The general arrangement of synaptic boutons observed in the initial and later images was similar for the 20 cells (15

Fig. 3. Comparison of nerve terminal maps over progressively longer times. **(Top)** Pattern of preganglionic endings derived from two focus-through series of the same neuron obtained 1 hour apart. Between the two series, the wound was closed and the animal removed from the setup; the mouse was then reanesthetized and repositioned on the focusing stage, and the ganglion once again mounted for viewing. Under these circumstances, some differences in the maps are evident. These discrepancies are presumably the result of differences in the geometrical disposition of the cell and its surroundings at the two different viewings. **(Middle)** Comparison of the nerve terminal maps derived from another ganglion cell observed at an interval of 7 days. The differences in the maps after 1 week tended to be greater than the differences between maps obtained after 1 hour (see also Fig. 4B). **(Bottom)** Comparison of the nerve terminal maps of the surface of another ganglion cell observed at an interval of 23 days (see also Fig. 4A). Substantial differences between the two maps were seen more often after 3 weeks than after 1 week (Fig. 4B). The index of similarity (see Fig. 4) was 0.77 for the pair of images in (top), 0.60 for (middle), and 0.42 for (bottom). These values are close to the means shown in Fig. 4.



animals) examined in this way (Fig. 3, top, and Fig. 4).

To quantitate differences in the images, we calculated an index of similarity for the pattern of synaptic staining in the two neuronal maps (Fig. 4A). The maps of the neuronal surface were divided into an array of squares measuring 32 pixels on a side. Each square was assigned an intensity proportional to the amount of terminal staining within it. The index of similarity between the initial and final images was then obtained by computing a correlation coefficient, which compared the intensities of corresponding squares (12). The similarity values for neuronal maps obtained an hour apart—a period that we again assume to be too brief for significant biological change to occur—are thus the baseline against which changes over longer intervals must be judged (Fig. 4B).

After a week, the differences in the configuration of synapses on 22 identified ganglion cells (17 animals) that were imaged a second time appeared to be somewhat greater (Fig. 3, middle). Quantitative analysis of the initial and final patterns confirmed that the differences in the two maps after a week

were, on the average, increased over the baseline values observed after an interval of an hour (Fig. 3, middle, and Fig. 4). To determine whether this phenomenon is progressive, a further 23 neurons (15 animals) were examined at an interval of 3 weeks. The differences among the fluorescence patterns on the surfaces of identified cells after 3 weeks were greater than the differences observed after 1 week (Fig. 3, bottom, and Fig. 4). On the average, the sum of the number of pixels representing nerve terminals in the initial and final images did not change appreciably over any of these intervals; thus there was no indication of a net gain or loss of synapses among the population of neurons studied over periods of up to 3 weeks.

The significance of the work that we report here is twofold. First, these methods allow visualization of synaptic terminals on living nerve cells. This approach may be useful elsewhere in the nervous system. After administration of dye, stained elements that may represent nerve endings were also apparent in sympathetic ganglia, in enteric ganglia, in the cornea, and in some regions of the central nervous system. Second, our

results suggest an ongoing rearrangement of interneuronal synapses in maturity.

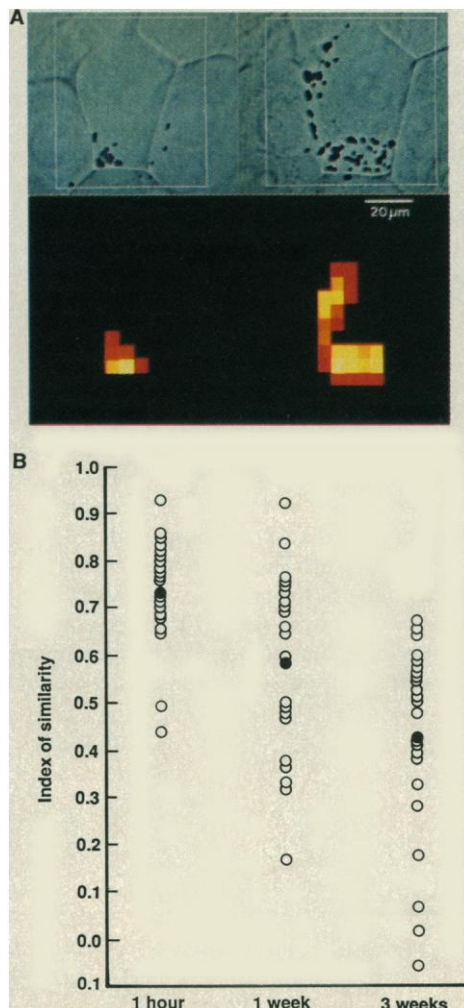
Because this latter conclusion has substantial implications, it is important to consider alternative explanations of our results. The changes in terminal configuration could be a consequence of damage from the staining and imaging procedures. Although we found no physiological or morphological evidence of synaptic dysfunction, we cannot rule out more subtle effects that might stimulate synaptic change over time. However, motor nerve endings in a nearby muscle stained topically with a related styryl pyridinium dye (4-Di-2-ASP) show relatively little change in synaptic configuration, even after several months (4, 5). The fact that motor nerve terminals on mammalian muscle fibers do not change after being subjected to the same procedures provides some assurance that the differences we describe here are the normal behavior of these interneuronal synapses. A second factor that might lead to an erroneous impression of synaptic change is incomplete imaging of nerve terminals on the surfaces of the target neurons at one or another of the operations. However, artifacts arising in this way should have influenced our results equally at all intervals and would not explain the apparently progressive nature of the changes that we observed. A third possibility is that the changes result from differences in the arrangement of the underlying neurons, rather than the arrangement of the nerve terminals on their surfaces. For example, because our maps were limited to the upper surfaces of the ganglion cells, we cannot be certain that these neurons (which lack dendrites) do not gradually rotate, bringing new sets of synapses into view and obscuring others. Although the stability of the neuronal outlines and neighbor relations [Fig. 3 (2, 3, 6)] make this possibility unlikely, we cannot rule it out.

There is no doubt that patterns of innervation in adult mammals can change in response to experimental perturbation (13). On the other hand, there is little evidence that this potential for change is realized under normal circumstances; the only well-documented example of physiological remodeling has been the amphibian neuromuscular junction (14). Our results, together with our earlier observations on the malleability of autonomic ganglion cell dendrites (2, 3), indicate that connections between nerve cells in mature mammals may be considerably more dynamic than has generally been thought.

REFERENCES AND NOTES

1. D. Purves and J. Voyvodic, *Trends Neurosci.* 10, 398 (1987).
2. D. Purves and R. D. Hadley, *Nature (London)* 315,

Fig. 4. Quantitative differences among nerve terminal maps for the entire population of cells studied over intervals of up to 3 weeks (of the 69 cells examined, 4 were omitted from the analysis because of inadequate quality of either the initial or final image). (A) Method of comparing maps, exemplified here by a neuron examined at an interval of 3 weeks. To systematically evaluate the differences in the disposition of synapses on the same cell at two different times, an index of similarity between the initial and final maps was determined. Because the location, rotation, and magnification of the initial and final images of the same cell were always slightly different, the cell outline obtained at the second observation was aligned and scaled so that it conformed as closely as possible to the cell outline initially observed. This procedure brought corresponding parts of the two neuronal surface images into approximate register. The two images were then divided into a 16 by 16 array of squares, 32 pixels on a side; the intensity of each square (lower panels) corresponds to the proportion of pixels in it that represent the preganglionic endings (upper panels). Intensities were scaled from 0 to 255, with yellow representing the maximum intensity and red the minimum non-0 intensity. The index of similarity (which is 0.51 for this particular set of maps) was then obtained by computing a correlation coefficient of the corresponding boxes in the two images by means of a linear regression model (15). A similarity index of 1.0 indicates perfect correspondence of the two maps; an index of 0 indicates no detectable similarity. (B) Similarity indices of nerve terminal maps on identified neurons obtained at intervals of 1 hour, 1 week, and 3 weeks. Over several weeks, the similarity of the initial and final synaptic patterns became progressively less. Each open circle represents a single cell, monitored over the indicated interval; the filled circles represent the mean index values at each interval.



- 404 (1985).
3. ———, J. Voyvodic, *J. Neurosci.* **6**, 1051 (1986).
 4. L. Magrassi, D. Purves, J. W. Lichtman, *ibid.* **7**, 1207 (1987).
 5. J. W. Lichtman, L. Magrassi, D. Purves, *ibid.*, p. 1215.
 6. D. Purves and J. W. Lichtman, *ibid.*, p. 1492.
 7. W. D. Snider, *ibid.*, p. 1760.
 8. J. W. Lichtman, *J. Physiol. (London)* **273**, 155 (1977).
 9. J. Voyvodic, *Soc. Neurosci. Abstr.* **12**, 390 (1986).
 10. R. Hume and D. Purves, *J. Physiol. (London)* **338**, 259 (1983).
 11. C. J. Forehand and D. Purves, *J. Neurosci.* **4**, 1 (1984).
 12. Correlation of pairs of composite maps on a pixel by pixel basis was not routinely done because such a detailed analysis emphasizes apparent differences in the two maps that are, in fact, below the resolving power of our imaging technique.
 13. C. W. Cotman, M. Nieto-Sampedro, E. W. Harris, *Physiol. Rev.* **61**, 684 (1981); M. C. Brown, R. L. Holland, W. G. Hopkins, *Annu. Rev. Neurosci.* **4**, 17 (1981); L. Mendell, *Physiol. Rev.* **64**, 260 (1984); D. Purves and J. W. Lichtman, *Principles of Neural Development* (Sinauer, Sunderland, MA, 1985).
 14. A. Wernig and A. A. Herrera, *Prog. Neurobiol.* **27**, 251 (1986); A. A. Herrera and L. R. Banner, *Soc. Neurosci. Abstr.* **13**, 1665 (1987).
 15. O. Ostle and R. W. Mensing, *Statistics in Research* (Iowa State Univ. Press, Ames, ed. 3, 1975), p. 237.
 16. We thank W. J. Sunderland for his expert help with various aspects of the image processing and graphic analysis procedures and C. J. Forehand, L. Harris, S. L. Pomeroy, and J. R. Sanes for helpful comments on the manuscript.

6 May 1987; accepted 6 October 1987

A New Prosomatostatin-Derived Peptide Reveals a Pattern for Prohormone Cleavage at Monobasic Sites

ROBERT BENOIT,* NICHOLAS LING, FREDERICK ESCH

Cleavage of the peptide bonds of preprosomatostatin at basic residues near the carboxyl terminus yields somatostatin-14, somatostatin-28, and somatostatin-28(1-12). However, little is known about the molecular forms derived from the amino terminal portion of the precursor, even though this part of the prohormone is highly conserved through evolution. By using an antibody against the amino terminus of prosomatostatin, a decapeptide with the structure Ala-Pro-Ser-Asp-Pro-Arg-Leu-Arg-Gln-Phe, corresponding to preprosomatostatin(25-34), was isolated from the endocrine portion of the rat stomach, the gastric antrum. The antral decapeptide may represent a bioactive product generated from prosomatostatin after a monobasic cleavage similar to that involved in the formation of somatostatin-28. In fact, a monobasic cleavage requires two basic residues and a domain containing nonpolar amino acids such as alanine or leucine, or both.

PEPTIDES DESTINED FOR SECRETION from cells are derived from precursor proteins by post-translational modifications. Most important among these modifications are the enzymatic cleavages that usually occur at some dibasic residues and occasionally at monobasic sites. The primary structure of neurohormone precursors can be elucidated rapidly by recombinant DNA technology. It then becomes important to predict how these precursors are processed in order to identify the new peptide products derived from the prohormones.

The somatostatin precursor is a useful model for studying neuropeptide processing in mammals, largely because of its simplicity. A single gene codes for the 92-amino acid prohormone (1). The precursor is not glycosylated, and contains only one pair of

basic amino acids (preceding somatostatin-14) and no repetitive sequences. The region of the prohormone endowed with the pan-inhibitory activity corresponds to the cyclic structure formed by its last 12 amino acids (2). Since the identification of the somatostatin precursor, we have been searching for additional bioactive domains contained in the 80-amino acid sequence preceding the carboxyl terminal dodecapeptide. Using antibody probes directed toward the carboxyl terminus of the precursor, we have identified two peptides derived from prosomatostatin (3, 4) that do not contain the original tetradecapeptide somatostatin: somatostat-

in-28(1-12) and preprosomatostatin(25-100). Even though these two peptides have been established as secretory products and are widely distributed in brain and digestive system, no biological role has been ascribed to them (5).

The presence of somatostatin-28 and somatostatin-28(1-12) in tissue extracts indicates that classic cleavage at a pair of basic amino acids is not the sole type of peptide hydrolysis during processing of prosomatostatin (6, 7). Cleavage at the monobasic site Arg⁸⁸-Ser⁸⁹ also occurs (Fig. 1). Recently, efforts have been directed toward the identification of putative peptides derived from the amino terminus of prosomatostatin (4, 5, 8, 9). Using an antibody directed toward the preprosomatostatin(25-33) segment, we have screened tissues of adult rats for the presence of preprosomatostatin(25-33)-like material (10) with a radioimmunoassay (RIA). The hypothalamus and the stomach contained the highest concentration of immunoreactive material (9.1 ± 1.4 and 6.2 ± 0.5 ng per 100 mg of wet weight, respectively; mean ± SEM; n = 10 rats). When this material was subjected to gel permeation chromatography, the stomach was found to contain an immunoreactive 1.2- to 1.4-kD species that was virtually absent in brain, pancreas, and duodenum. Thus differential processing occurred at the amino terminus of prosomatostatin. Here we describe the isolation and characterization of the 1.4-kD peptide. In addition, we propose a new processing scheme to account for the derivation of the peptide from prosomatostatin.

Stomachs from three Sprague-Dawley rats were collected and the corpus, antrum, and cutaneous region dissected (11) and extracted in 2M acetic acid containing peptidase inhibitors. RIA measurements were performed on the extract or on the fractions eluted from Sephadex G-75 gel permeation chromatography columns (Fig. 2).

Immunoreactivity in the cutaneous zone was low (total content per stomach, 2 ng). The corpus of the stomach contained 18.5 ng of preprosomatostatin(25-33)-like immunoreactive material of which 14.3 ng eluted from the gel permeation column as large molecular forms and 4.2 ng as a molec-

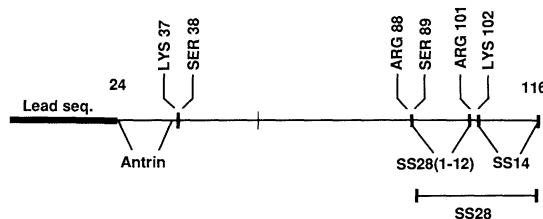


Fig. 1. Schematic representation of 116-amino acid mammalian preprosomatostatin, which includes the tetradecapeptide somatostatin-14 (SS14), somatostatin-28 (SS28), somatostatin-28(1-12) [SS28(1-12)], the amino terminal peptide antrin, and the 24-amino acid leader sequence. The three main cleavage points of the prohormone at positions 101-102, 88-89, and, conceivably, 37-38 are shown.

R. Benoit, Montreal General Hospital Research Institute, Department of Medicine, McGill University, Montreal, Quebec H3G 1A4, Canada.
N. Ling and F. Esch, Laboratories for Neuroendocrinology, Salk Institute, La Jolla, CA 92138.

*To whom correspondence should be addressed.